NASA SP-8032

VEHICLE
N CRITERIA
(STRUCTURES)

BUCKLING OF THIN-WALLED DOUBLY CURVED SHELLS

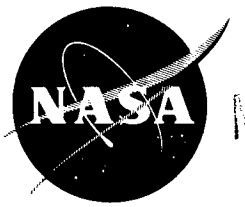

AUGUST 1969

NATIONAL AERONAUTICS AND SPACE ADMINISTRATION

FOREWORD

NASA experience has indicated a need for uniform criteria for the design of space vehicles. Accordingly, criteria are being developed in the following areas of technology:

Environment

Structures

Guidance and Control

Chemical Propulsion.

Individual components of this work will be issued as separate monographs as soon as they are completed. A list of all previously issued monographs in this series can be found at the end of this document.

These monographs are to be regarded as guides to design and not as NASA requirements, except as may be specified in formal project specifications. It is expected, however, that the criteria sections of these documents, revised as experience may indicate to be desirable, eventually will become uniform design requirements for NASA space vehicles.

This monograph was prepared under the cognizance of the Langley Research Center. The Task Manager was A. L. Braslow. The authors were V. I. Weingarten and P. Seide of the University of Southern California. A number of other individuals assisted in developing the material and reviewing the drafts. In particular, the significant contributions made by B. O. Almroth of Lockheed Missiles & Space Company, E. H. Baker of California Polytechnic Institute, D. O. Brush of the University of California at Davis, R. F. Crawford of Astro-Research Corporation, G. A. Greenbaum of TRW Systems, R. E. Hubka of Lockheed-California Company, R. R. Meyer of McDonnell Douglas Corporation, M. D. Musgrove of The Boeing Company, J. P. Peterson of NASA Langley Research Center, and G. A. Thurston of Martin Marietta Corporation are hereby acknowledged.

Comments concerning the technical content of these monographs will be welcomed by the National Aeronautics and Space Administration, Office of Advanced Research and Technology (Code RVA), Washington, D.C. 20546.

August 1969

CONTENTS

BUCKLING OF THIN-WALLED DOUBLY CURVED SHELLS

1. INTRODUCTION

Doubly curved shells are frequently used as walls of space vehicles and as external closures or internal common bulkheads in fuel tanks. When doubly curved shells develop compressive membrane forces in reaction to externally applied loads, their load-carrying capacity is often limited by structural instability, or buckling. In many cases, this capacity or buckling strength of a shell is reached when slight increases in the external loading produce large and abrupt changes or buckles in the surface geometry of the shell. For shells which do not fail catastrophically, a further increase in the external loading will gradually produce amplification of buckles, accompanied by plastic deformation that eventually results in collapse of the structure.

The buckling strength of a doubly curved shell depends upon its curvature, its geometric proportions (including the stiffening, when present), the elastic properties of its materials, the manner in which its edges are supported, and the nature of the applied loading. Initial, although small, geometric deviations of the shell from its ideal shape can have a significant adverse effect on the buckling strength of doubly curved shells, and can cause large scatter of experimental results.

This monograph presents criteria and recommends practices for design of compressively loaded doubly curved shells. Data are given for shells of revolution, including complete spheres, ellipsoids, and toroids, as well as for bulkheads. Most of the data are for shells subjected to uniform pressure loads, although data are also given for point loads on spheres.

The reduction of critical buckling loads caused by imperfections, small dynamic oscillations, boundary conditions, and the like is usually accounted for by multiplying the theoretical buckling loads by a correlation factor to obtain a lower-bound conservative estimate. However, when insufficient data are available to obtain correlation factors, testing is recommended to verify the design. Experimental verification is also recommended for shells of arbitrary shape and for shells of revolution having cutouts, joints, plasticity effects, and nonuniform shell stiffness. The effect of small oscillations in applied loading is considered to be accounted for by the correlation factor.

Related subjects include buckling of circular cylindrical shells (ref. 1) and buckling of truncated conical shells (ref. 2), as well as buckling strength of structural plates, which is to be treated in a planned NASA monograph. An ultimate design factor is used in estimating design loads for buckling. Considerations involved in selecting the numerical value of this factor are to be presented in another planned NASA monograph.

2. STATE OF THE ART

The buckling strength of shells is usually determined by combining theoretical predictions with experimentally determined correlation factors. For doubly curved shells, considerable capability for theoretical analysis is available. Experimental investigations of the stability of doubly curved shells, however, lag far behind analytical capabilities; the shallow spherical cap under external pressure is the only problem which has been investigated extensively.

Eccentricity effects (i.e., "onesidedness") of stiffened shells cannot usually be neglected in buckling investigations. When eccentricity is included, significant differences can be obtained in buckling loads for some shell geometries. Numerical results given in reference 3 also show that theory based upon membrane-prebuckling analysis can give different results than theory based on the more comprehensive linear- or nonlinear-bending prebuckling analysis. Dynamic loading may also lower the static buckling strength of shells.

Until quite recently, most theoretical stability studies of doubly curved shells were limited to spherical shells subjected to simplified loading conditions and with simplified edge restraints. The growing use of digital computers for analysis of shell structures has improved this situation, although not all restrictions have been removed. For example, available finite-difference computer programs for doubly curved shells are limited to elastic analysis of orthotropic shells of revolution with constant elastic stiffness as shown in reference 3, and to isotropic layered construction (ref. 4). These programs are suitable for use in design of shells of double curvature if complemented by tests that provide a suitable correlation factor.

The program of reference 3 computes the buckling loads of shells of revolution for either membrane or nonlinear prebuckling bending stresses resulting from axisymmetric loadings of constant axial compression and uniform external pressure. Because of approximations in the theory, buckling loads for shells with rapid changes of curvature of the meridian or for shells which buckle with a small number of circumferential waves cannot be obtained accurately. Stiffened shells may be analyzed if the stiffening elements are so closely spaced that they may be smeared out. Stiffened shells are generally more efficient and less sensitive to imperfections. The results of the program may be complemented by studies similar to those of references 5 to 8 which permit an estimate of the effect of initial imperfections on buckling strength. For shells which such studies show to be insensitive to imperfections, fewer tests are required to establish design values.

The program of reference 4 permits the nonlinear analysis of shells of revolution under asymmetric surface and thermal loading, but cannot indicate the possibility of the existence of another nonlinear state at some value of the load. The maximum number of meridional node points is 20 and the maximum number of circumferential Fourier components is 10. Boundary conditions may be closed at one or both ends, or may be free, fixed, or elastically restrained. This program may be used to obtain buckling loads defined by the maximum load for which equilibrium can be maintained.

A number of programs similar to that described in reference 3, but which use a finite-element approach, have been developed and appear to be promising. However, these are not documented nor generally available. All the programs for doubly curved shells, including both finite-difference and finite-element, treat only those cases where the shell does not become plastic prior to buckling.

Although the capability for stability analysis has increased, there is a lack of parametric optimization studies for problems of interest. This may well be due to the relative newness of most computer programs. To date, most computer programs have been used for spot checks of approximate solutions and for comparisons with experimental data.

Available design information is summarized in Section 4. To put improved procedures to immediate use, however, the designer is advised to be alert to new developments in shell-stability analysis. The recommendations will be modified as more theoretical and test data become available.

3. CRITERIA

3.1 General

Structural components consisting of thin, curved isotropic or composite sheet, with or without stiffening, shall be so designed that (1) unanticipated buckling resulting in collapse of the structural components will not occur from the application of ultimate design loads, and (2) buckling deformation resulting from limit (maximum expected) loads will not be so large as to impair the function of the structural components or nearby components, nor so large as to produce undesirable changes in loading.

3.2 Guides for Compliance

Design loads for buckling shall be considered to be any combination of ground or flight loads, including loads resulting from temperature changes, that cause compressive

inplane stresses (multiplied by the ultimate design factor) and any load or load combination tending to alleviate buckling (not multiplied by the ultimate design factor). Buckling strength of thin-walled doubly curved shells shall be defined by analyses which include semiempirical correlation factors.

Representative structures shall be tested under conditions simulating the design loads when:

- Configurations are shells of arbitrary shape.
- Configurations are of minimum weight, and coupling between the various modes of failure is possible.
- No theory or correlation factor exists.
- Correlation factors used are less conservative than those recommended in this document.
- Cutouts, joints, or other design irregularities occur.

4. RECOMMENDED PRACTICES

4.1 Scope

Procedures for the estimation of buckling loads on doubly curved shells are described in this section; the source of the procedures and limitations of the procedures are discussed. Where the recommended practice is suitably defined in all its detail in a readily available reference, it is merely outlined.

4.2 Isotropic Doubly Curved Shells

Unstiffened isotropic doubly curved shells subjected to various conditions of loadings are considered in this section. Solutions are limited to spherical, ellipsoidal, and toroidal shells.

4.2.1 Spherical Shells

4.2.1.1 Spherical Caps Under Uniform External Pressure

The buckling of a spherical cap under uniform external pressure (fig. 1) has been treated extensively. Theoretical results are presented in references 9 and 10 for

axisymmetric snap-through of shallow spherical shells with edges that are restrained against translation, but are either free to rotate or are clamped. Results for asymmetric buckling are given in references 11 and 12 for the same boundary conditions. The results reported in these references are presented as the ratio of the buckling pressure p_{cr} for the spherical cap and the classical buckling pressure $p_{c\ell}$ for a complete spherical shell as a function of a geometry parameter λ:

$$\frac{p_{cr}}{p_{c\ell}} = f(\lambda) \tag{1}$$

with

$$p_{c\ell} = \frac{2}{\left[3(1-\mu^2)\right]^{\frac{1}{2}}} E\left(\frac{t}{R}\right)^2 \tag{2}$$

$$\lambda = \left[12(1-\mu^2)\right]^{\frac{1}{4}} \left(\frac{R}{t}\right)^{\frac{1}{2}} 2\sin\frac{\phi}{2} \tag{3}$$

where ϕ is half the included angle of the spherical cap (fig. 1).

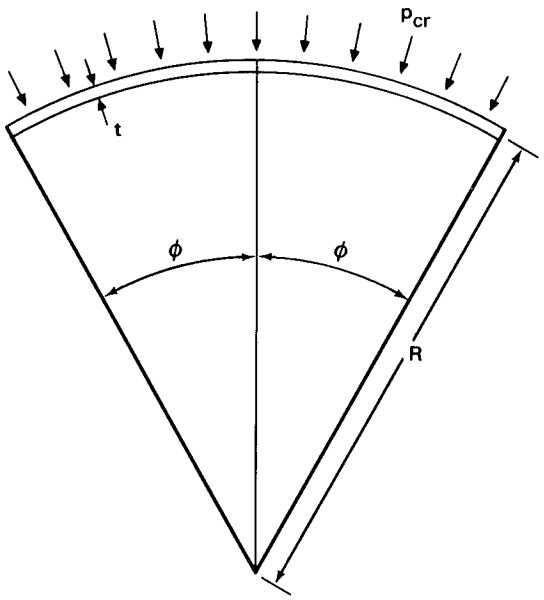

Figure 1
Geometry of spherical cap under uniform external pressure

The function $f(\lambda)$ depends on the boundary conditions imposed on the shell.

Most of the available test data apply to spherical shells, and values are lower than theoretically predicted buckling pressures. The discrepancy between theory and experiment can be largely attributed to initial deviations from the ideal spherical shape

(refs. 10, 13, and 14) and to differences between actual and assumed edge conditions (refs. 15 and 16). Most of the available data are summarized in reference 17; some other test results are given in references 13 and 18. A lower bound to the data for clamped shells is given by

$$\frac{p_{cr}}{p_{c\ell}} = 0.14 + \frac{3.2}{\lambda^2} \quad (\lambda > 2) \tag{4}$$

which is plotted in figure 2. While the λ parameter is used in shallow-shell analysis, figure 2 may be applied to deep shells as well as to shallow shells.

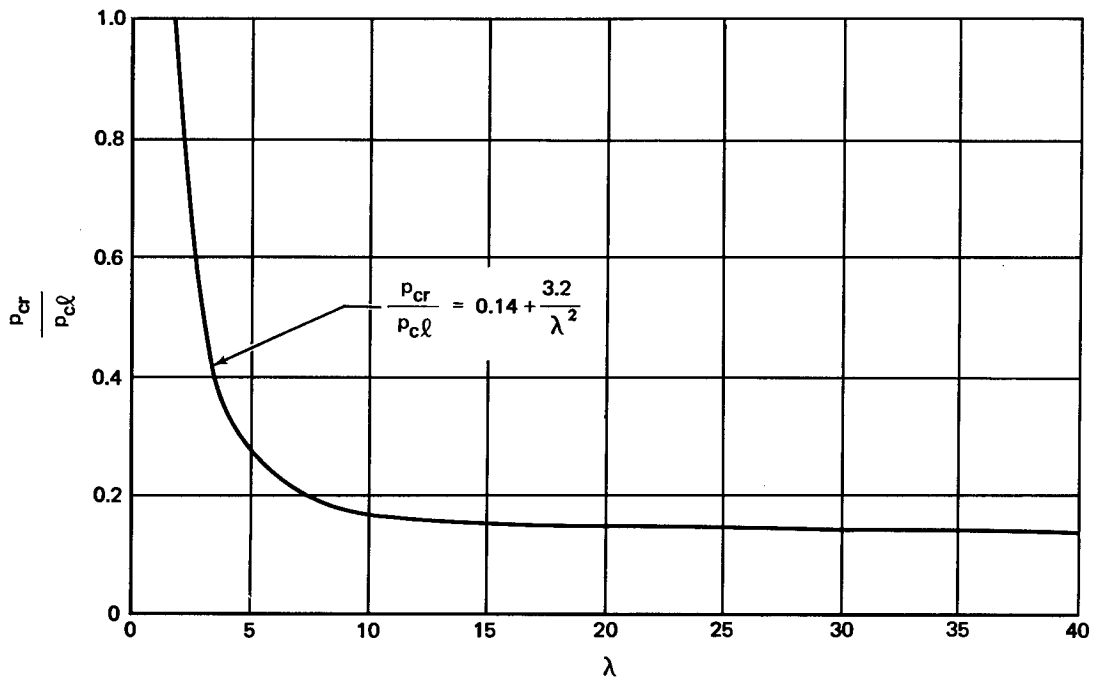

Figure 2.
Recommended design buckling pressure of spherical caps

4.2.1.2 Spherical Caps Under Concentrated Load at the Apex

Spherical caps under concentrated load at the apex (fig. 3) will buckle under certain conditions. Theoretical results for edges that are free to rotate and to expand in the direction normal to the axis of revolution and for clamped edges are given in reference 19 for axisymmetric snap-through and in references 7 and 20 for asymmetric buckling. Experimental results for loads which approximate concentrated loading are described in references 21 to 25.

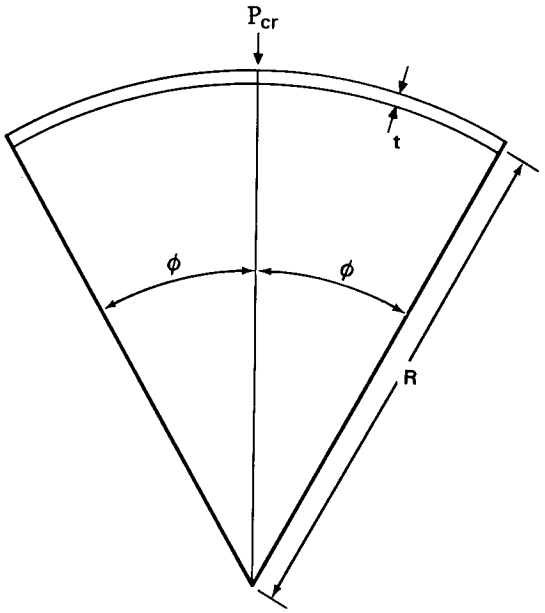

Figure 3
Geometry of spherical cap under concentrated load at the apex

For shells with unrestrained edges, buckling will not occur if λ is less than about 3.8. In this range of shell geometry, deformation will increase with increasing load until collapse resulting from plasticity effects occurs. For shells with values of λ greater than 3.8, theoretical and experimental results are in good agreement for axisymmetric snap-through, but disagree when theory indicates that asymmetric buckling should occur first. In this case, buckling and collapse are apparently not synonymous, and only collapse loads have been measured. A lower-bound relationship between the collapse-load parameter and the geometry parameter for the data of references 7, 21, and 22 for shells with unrestrained edges is given by

$$\frac{P_{cr}R}{Et^3} = \frac{1}{24}\lambda^2 \quad (4 \leqslant \lambda \leqslant 18) \tag{5}$$

For spherical caps with clamped edges, theory indicates that buckling will not occur if λ is less than about 8. For values of λ between 8 and 9, axisymmetric snap-through will occur, with the shell continuing to carry increasing load. For larger values of λ, asymmetrical buckling will occur first, but the shell will continue to carry load. Although imperfections influence the initiation of symmetric or asymmetric buckling, few measurements have been made of the load at which symmetric or asymmetric deformations first occur. Experimental results indicate that the collapse loads of clamped spherical caps loaded over a small area are conservatively estimated by the loads calculated in reference 7 and shown in figure 4. When the area of loading becomes large, local buckling may occur at a lower load.

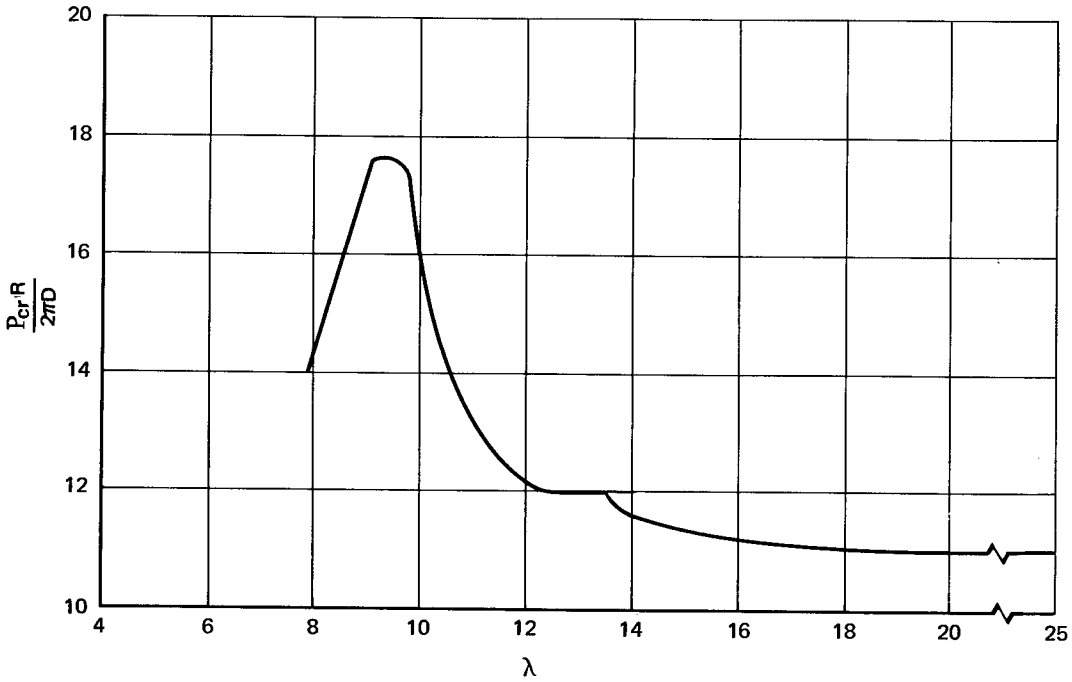

Figure 4
Theoretical buckling loads for clamped spherical cap under concentrated load

4.2.1.3 Spherical Caps Under Uniform External Pressure and Concentrated Load at the Apex

Clamped spherical caps subjected to combinations of uniform external pressure and concentrated load at the apex are discussed in reference 26. The experimental and theoretical data given there are insufficient, however, to yield conclusive results. A straight-line interaction curve is recommended:

$$\frac{P}{P_{cr}} + \frac{p}{p_{cr}} = 1 \qquad (6)$$

where P is the applied concentrated load, p the applied uniform pressure, P_{cr} the critical concentrated load given in Section 4.2.1.2, and p_{cr} is the critical uniform external pressure given in Section 4.2.1.1.

4.2.2 Ellipsoidal (Spheroidal) Shells

4.2.2.1 Complete Ellipsoidal Shells Under Uniform External Pressure

Ellipsoidal shells of revolution subjected to uniform external pressure, as shown in figure 5, are treated in reference 8. Calculated theoretical results for prolate spheroids

are shown in figures 6a and 6b. Experimental results given in reference 27 for prolate spherical shells with $4 > A/B > 1.5$ are in reasonably close agreement with the theoretical results of reference 8. For $A/B \geqslant 1.5$, the theoretical pressure should be multiplied by the factor 0.75 to provide a lower bound to the data. Results given in reference 28 for half of a prolate spheroidal shell ($A/B = 3$) closed by an end plate are in good agreement with those for the complete shell.

The analysis of reference 8 indicates that theoretical results for thin, oblate spheroidal shells are similar to those for a sphere of radius

$$R_A = \frac{B^2}{A} \tag{7}$$

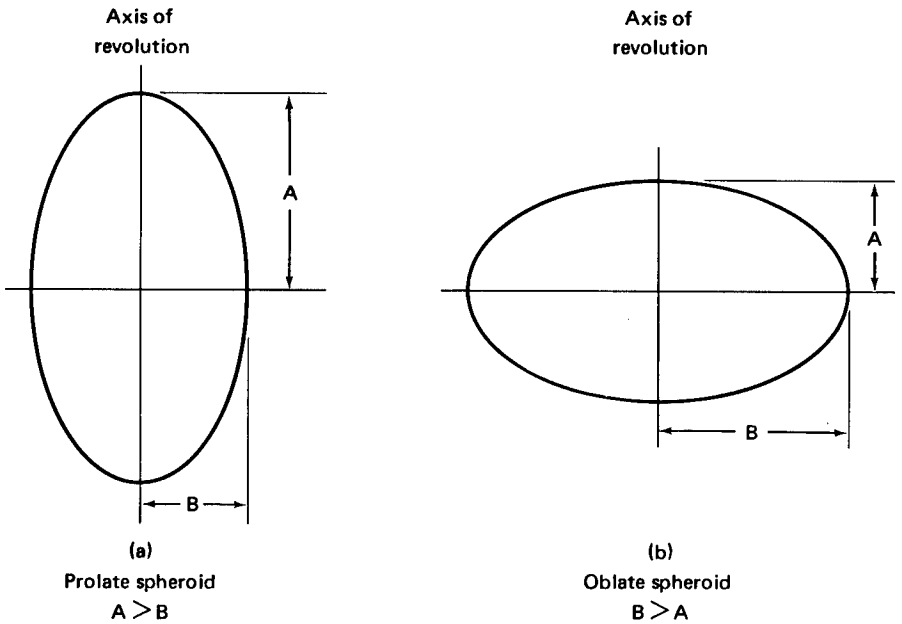

Figure 5
Geometry of ellipsoidal shells

The data of reference 29 show that experimental results are similar, as well. Thus, the external buckling pressure for a thin, oblate spheroid may be approximated by the relationship

$$\frac{\sqrt{3(1-\mu^2)}}{2}\left(\frac{R_A}{t}\right)^2 \frac{p}{E} = 0.14 \tag{8}$$

which is the limit of equation (4) as λ becomes large.

4.2.2.2 Complete Oblate Spheroidal Shells Under Uniform Internal Pressure

When the radius ratio A/B of an oblate spheroid is less than $\sqrt{\frac{2}{2}}$, internal pressure produces compressive stresses in the shell, and hence allows instability to occur. Theoretical values of the critical internal pressures given by the analysis of reference 8

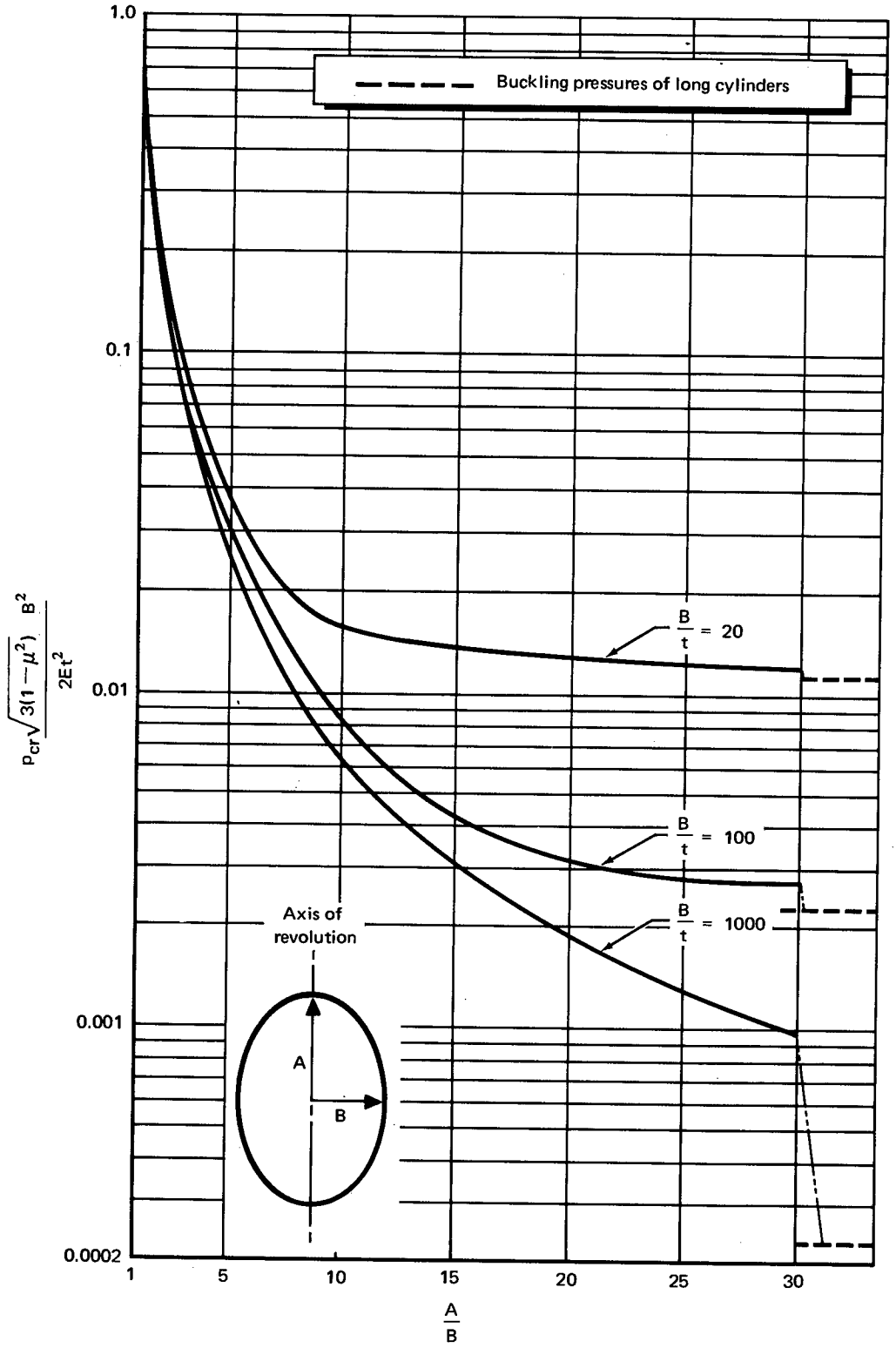

Figure 6a
Theoretical external buckling pressures of prolate spheroids (μ = 0.3)

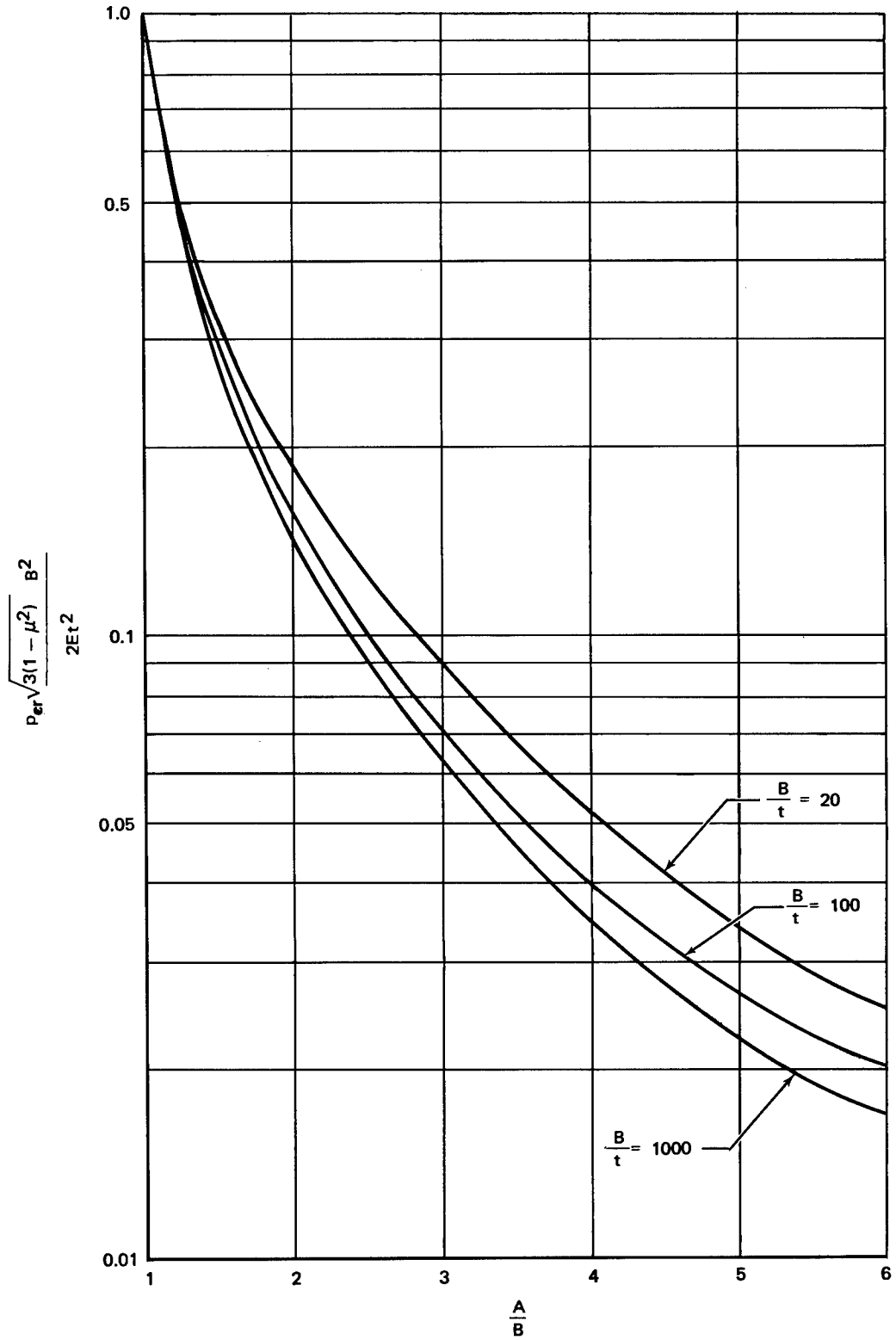

Figure 6b
Theoretical external buckling pressures of prolate spheroids (μ = 0.3)

are shown in figure 7. No experimental results are available, but the study of imperfection sensitivity of reference 8 indicates that there should be good agreement between theory and experiment for shells with $0.5 < A/B < 0.7$.

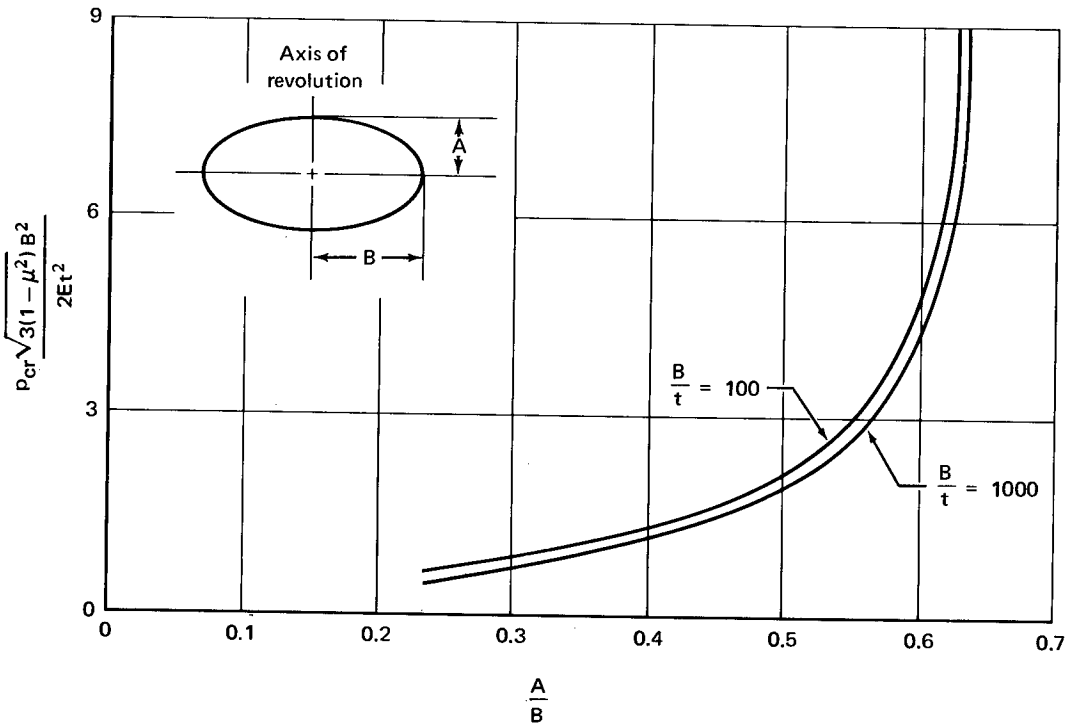

Figure 7
Theoretical buckling pressures of oblate spheroids under internal pressure (μ = 0.3)

4.2.2.3 Ellipsoidal and Torispherical Bulkheads Under Internal Pressure

Clamped oblate spheroidal (ellipsoidal) bulkheads (fig. 8) may have the ratio of length of minor and major axes (A/B) less than $\sqrt{\frac{2}{2}}$ without buckling under internal pressure, provided the thickness exceeds a certain critical value. This problem is investigated in reference 30. Nonlinear bending theory is used to determine the prebuckling stress distribution. The regions of stability are shown in figure 9; the calculated variation of buckling pressure with thickness is shown in figure 10. The theory has not been verified by experimental results, however, and should be used with caution.

Torispherical end closures, shown in figure 11, are also investigated in reference 30. Calculations are made for the prebuckling stress distribution in these bulkheads for ends restrained by cylindrical shells and for buckling pressures for torispherical

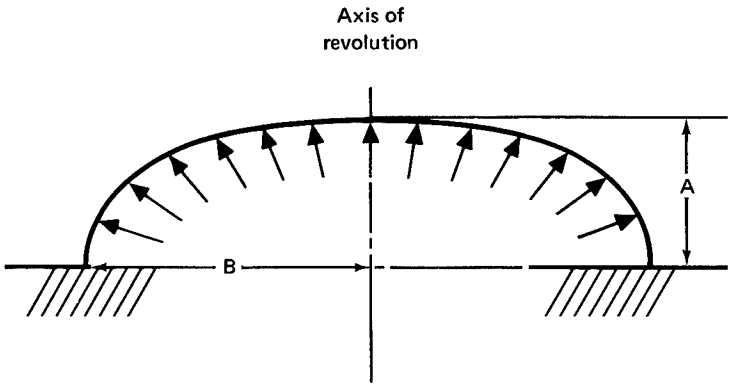

Figure 8
Clamped ellipsoidal bulkhead under internal pressure

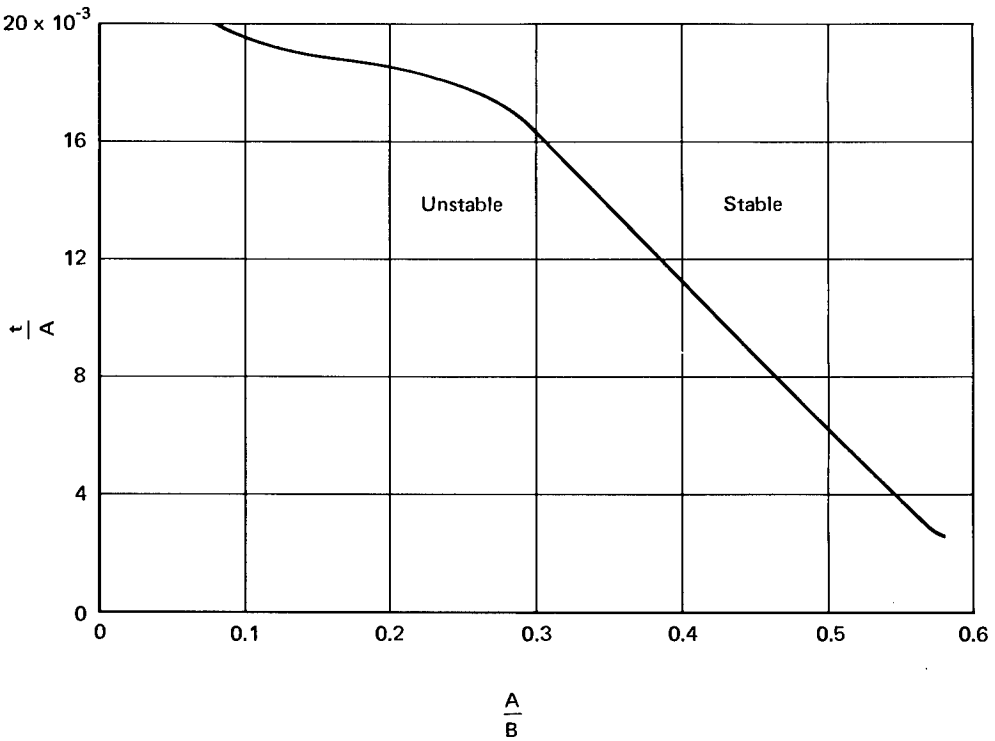

Figure 9
Region of stability for ellipsoidal closures subjected to internal pressure (μ = 0.3)

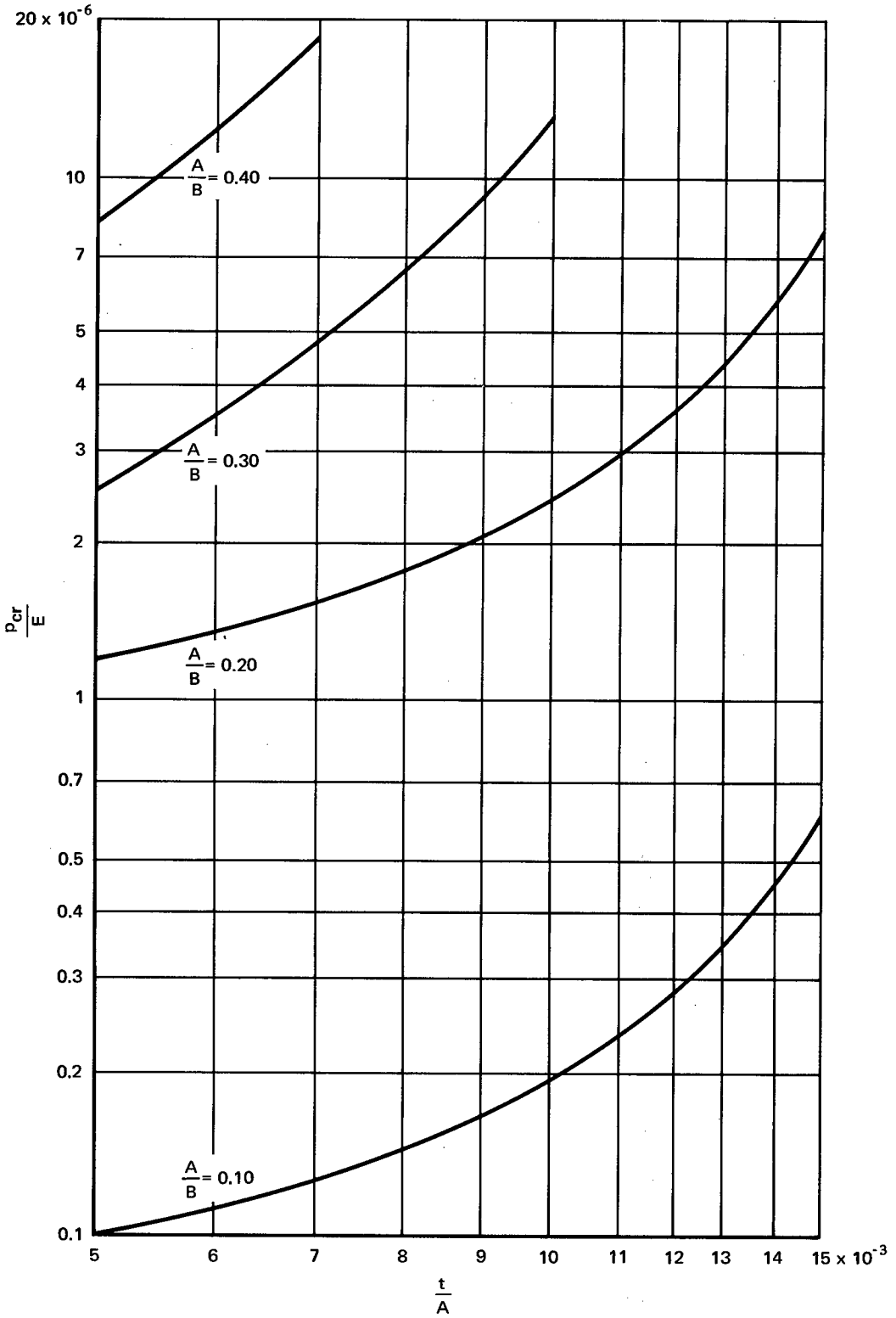

Figure 10
Theoretical results for clamped ellipsoidal bulkheads subjected to uniform internal pressure (μ = 0.3)

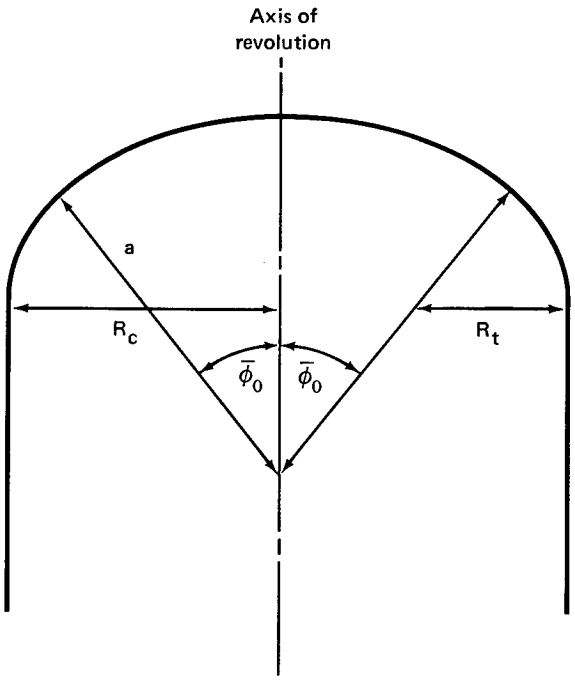

Figure 11
Geometry of torispherical closure

bulkheads with clamped edge conditions after buckling. The results are shown in figure 12. The experimental results of reference 31 indicate that the theoretically predicted buckling pressures should be multiplied by a correlation factor γ equal to 0.7.

4.2.3 Toroidal Shells

4.2.3.1 Complete Circular Toroidal Shells Under Uniform External Pressure

The complete circular toroidal shell under uniform external pressure (fig. 13) has been investigated and is described in reference 32; the theoretical results obtained are shown in figure 14.

Experimental results are given in reference 32 for values of b/a of 6.3 and 8, and indicate good agreement with theory. For values of b/a equal to or greater than 6.3,

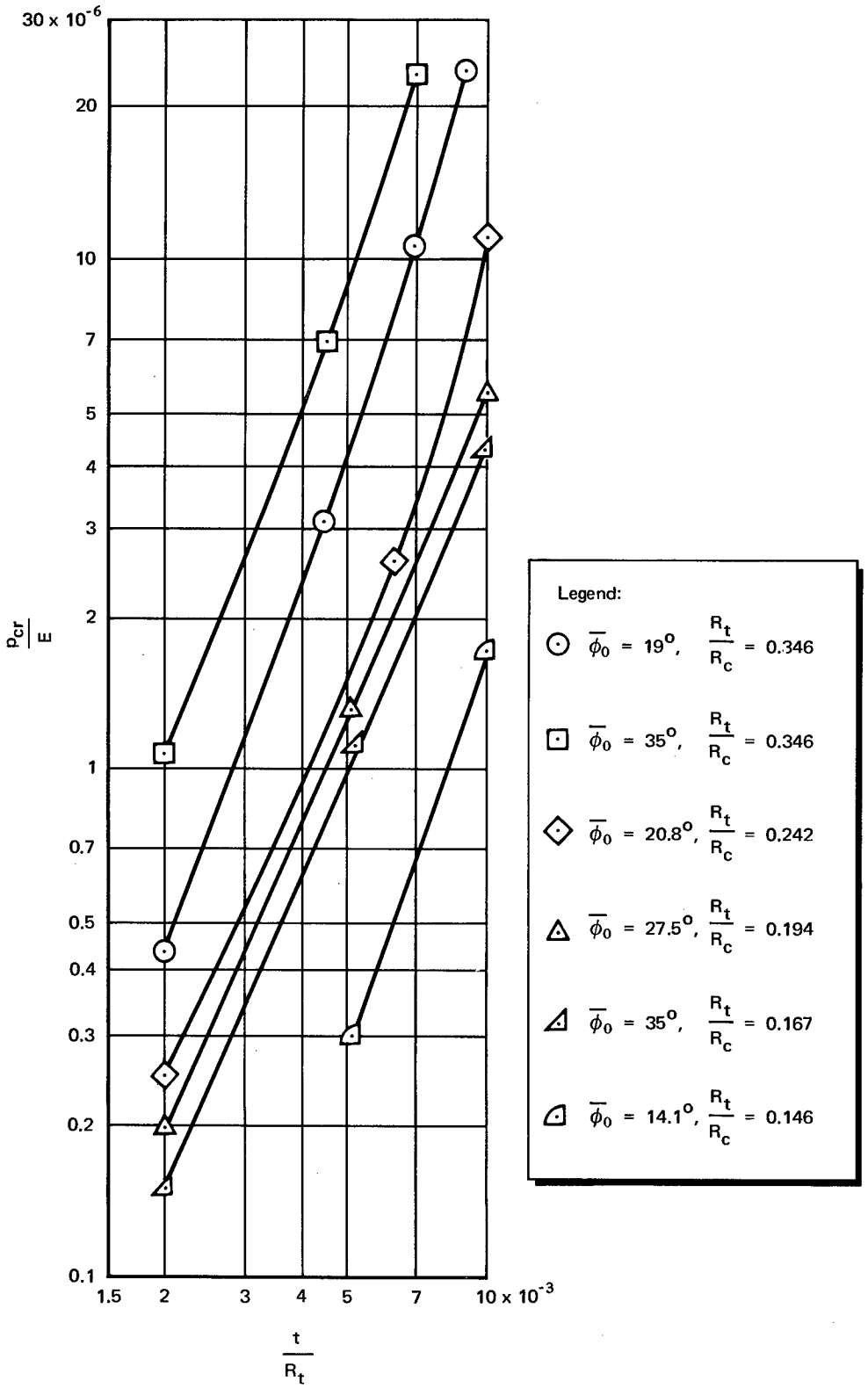

Figure 12
Theoretical results for torispherical closures subjected to uniform internal pressure (μ = 0.3)

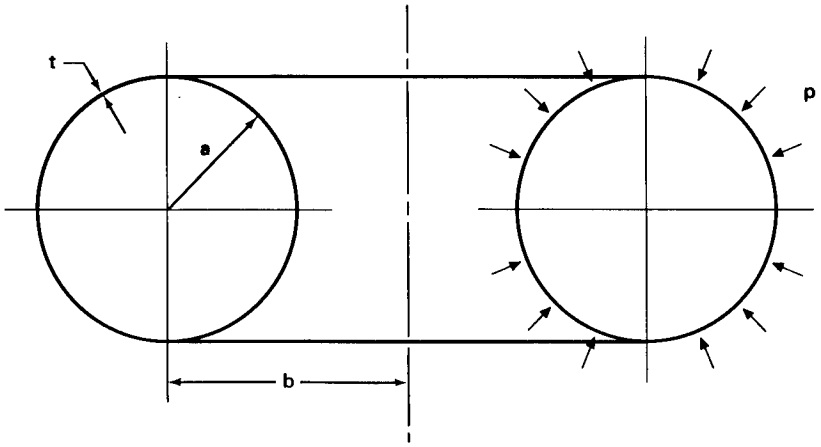

Figure 13
Geometry of a toroidal shell under uniform external pressure

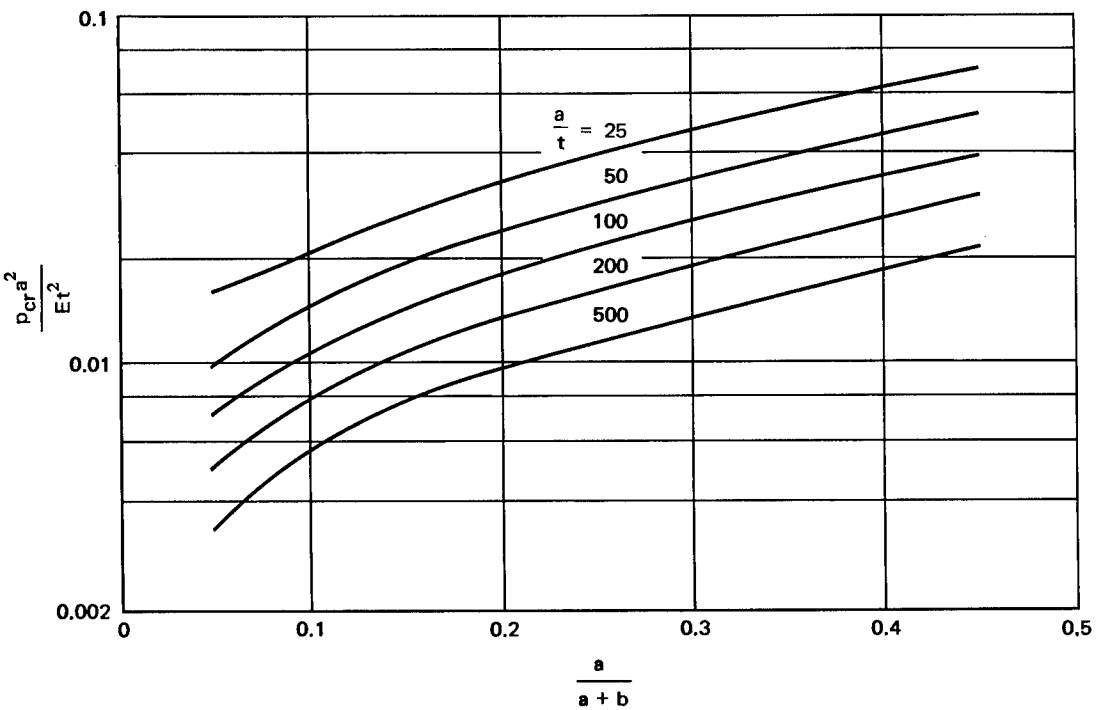

Figure 14
Theoretical buckling coefficients for toroidal shells under uniform external pressure

the theoretical buckling pressure should be multiplied by a factor of 0.9 to yield design values. This correction factor has been recommended in reference 1 for long cylindrical shells which correspond to a value of b/a of ∞. For values of b/a less than 6.3, the buckling pressure should be verified by test.

4.2.3.2 Shallow Bowed-Out Toroidal Segments Under Axial Loading

A bowed-out equatorial toroidal segment under axial tension (fig. 15) will undergo compressive circumferential stress and will thus be susceptible to buckling. An analysis for simply supported shallow segments is given in reference 33 and yields the relationship

$$\frac{N\ell^2}{\pi^2 D} = \frac{1}{\left(\frac{r}{a}\beta^2 - 1\right)}\left[(1+\beta^2)^2 + 12\frac{\gamma^2 Z^2}{\pi^4}\left(\frac{1+\frac{r}{a}\beta^2}{1+\beta^2}\right)^2\right] \qquad (9)$$

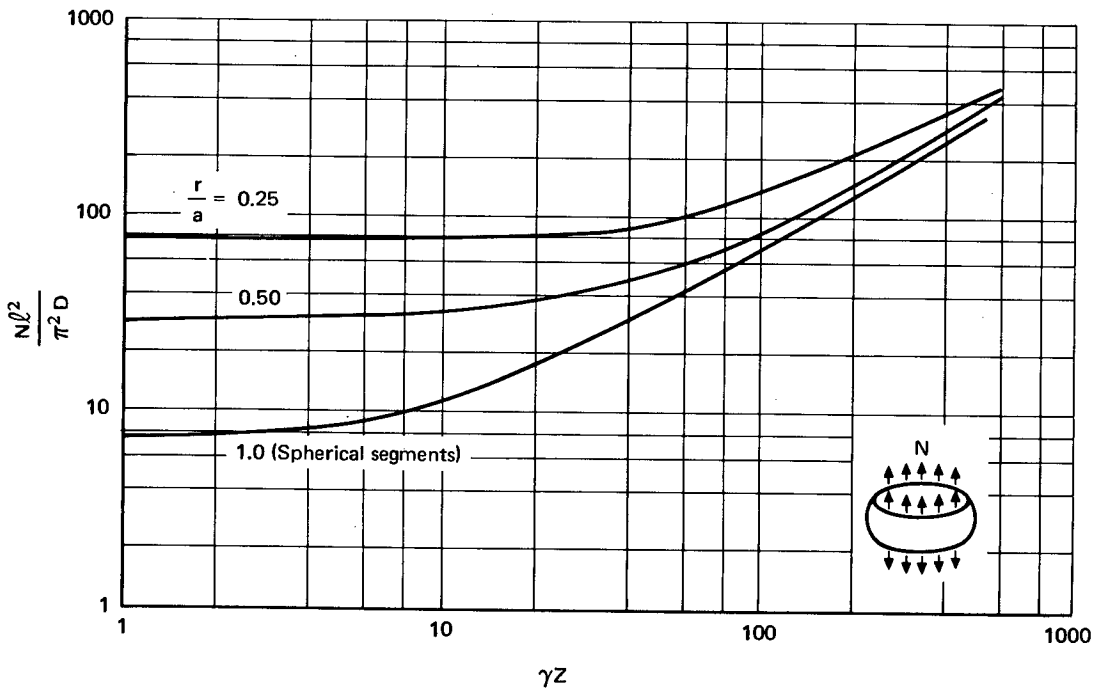

Figure 15.
Buckling of bowed-out toroidal segments under axial tension

where the correlation coefficient γ has been inserted to account for discrepancies between theory and experiment. The values obtained by minimizing equation (9) with respect to β are shown in figure 15. The straight-line portion of the curves are represented by the relationship

$$\frac{N\ell^2}{\pi^2 D} = \frac{4\sqrt{3}}{\pi^2}\gamma Z \tag{10}$$

A similar analytical investigation described in reference 34 for clamped truncated hemispheres in axial tension yields results in close agreement with those for the curve of figure 15 for r/a = 1.

Experimental results for the truncated hemisphere given in reference 34 indicate that the correlation coefficient for the curve for r/a equal to 1 is

$$\gamma = 0.35 \tag{11}$$

The same value of the correlation coefficient may be used for other values of r/a.

Some results for bowed-out equatorial toroidal segments under axial compression are given in reference 35; the equatorial spherical shell segment loaded by its own weight is treated in reference 36.

4.2.3.3 Shallow Toroidal Segments Under Uniform External Pressure

The term "lateral pressure" designates an external pressure which acts only on the curved walls of the shell and not on the ends; "hydrostatic pressure" designates an external pressure that acts on both the curved walls and the ends of the shell. Expressions for simply supported shallow equatorial toroidal segments subjected to uniform external lateral or hydrostatic pressure, as shown in figures 16 and 17, are given in reference 37 as

$$\frac{p_{cr} r\ell^2}{\pi^2 D} = \frac{1}{\beta^2}\left[(1+\beta^2)^2 + \frac{12}{\pi^4}\gamma^2 Z^2 \left(\frac{1 \pm \frac{r}{a}\beta^2}{1+\beta^2}\right)^2\right] \tag{12}$$

for lateral pressure, and as

$$\frac{p_{cr} r \ell^2}{\pi^2 D} = \frac{1}{\beta^2 \left(1 \mp \frac{1}{2}\frac{r}{a}\right) + \frac{1}{2}} \left[(1+\beta^2)^2 + \frac{12}{\pi^4} \gamma^2 Z^2 \left(\frac{1 \pm \frac{r}{a}\beta^2}{1+\beta^2} \right)^2 \right] \qquad (13)$$

for hydrostatic pressure. In equations (12) and (13), the upper sign refers to segments of type (a) of figure 18, while the lower sign refers to segments of type (b) of figure 18. The correlation coefficient γ has been introduced to account for discrepancies between theory and experiment. The results of minimizing the buckling pressure with respect to the circumferential wavelength parameter β are shown in figures 16 and 17. The straight-line portions of the curve for the shells of type (a) of figure 18 are represented by the relationships

$$\frac{p_{cr} r \ell^2}{\pi^2 D} = \frac{4\sqrt{3}}{\pi^2} \frac{r}{a} \gamma Z \qquad \text{(lateral pressure)} \qquad (14a)$$

$$\frac{p_{cr} r \ell^2}{\pi^2 D} = \frac{8\sqrt{3}}{2 - \frac{r}{a}} \frac{r}{a} \gamma Z \qquad \text{(hydrostatic pressure)} \qquad (14b)$$

No experimental data are available except for the cylindrical shell for which a correlation factor of

$$\gamma = 0.56 \qquad (15)$$

was recommended in reference 1. The same correlation factor can be used for shells with r/a near zero, but should be used with caution for shells of type (b) with values of r/a near unity. For shells of type (a) with values of r/a near unity, the shell can be conservatively treated as a sphere, or the buckling pressure should be verified by test.

4.3 Orthotropic Doubly Curved Shells

The term "orthotropic doubly curved shells" covers a wide variety of shells. In its strictest sense, it denotes single- or multiple-layered shells made of orthotropic materials. In this monograph, the directions of the axes of orthotropy for shells of revolution are assumed to coincide with the meridional and circumferential directions

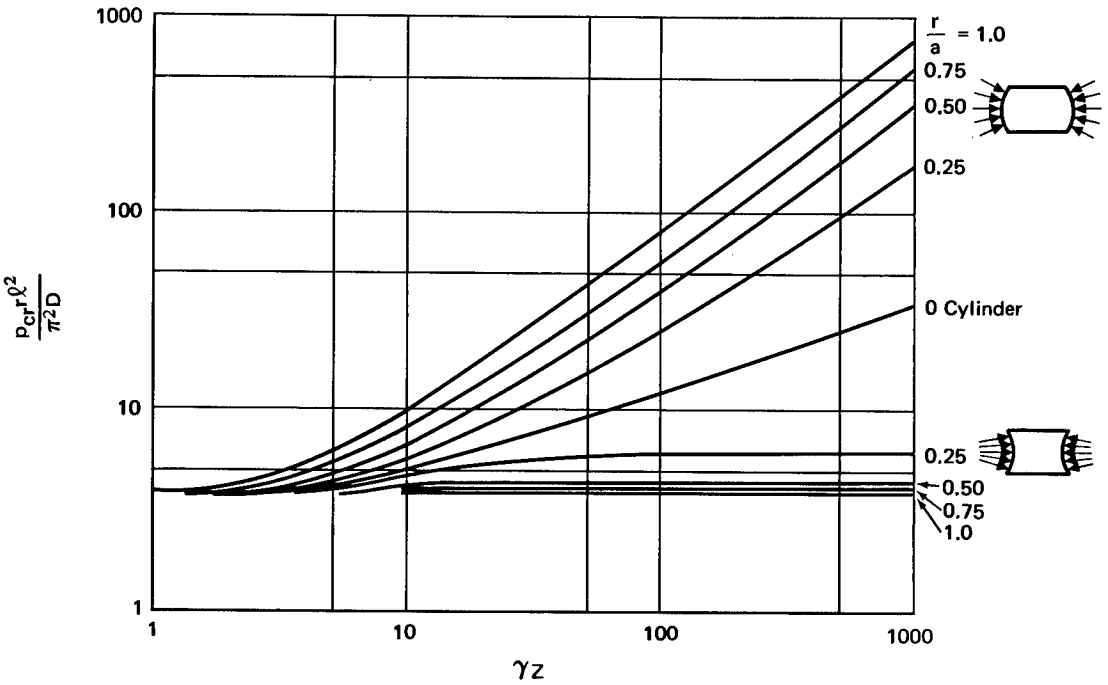

Figure 16.
Buckling of toroidal segments under uniform lateral pressure

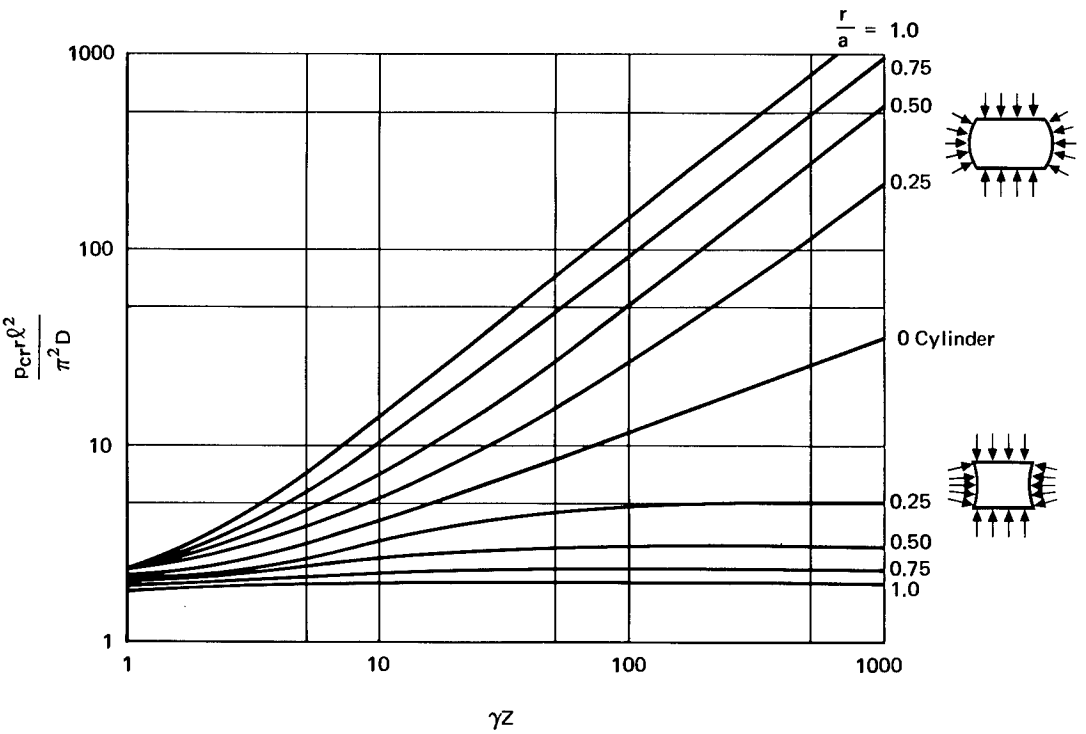

Figure 17
Buckling of toroidal segments under uniform external hydrostatic pressure

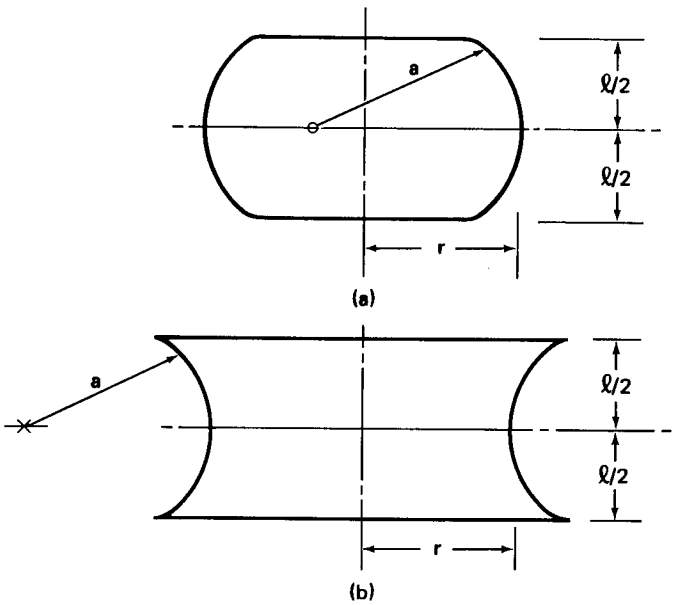

Figure 18
Geometry of toroidal segments near equators

of the shell. The term also denotes types of stiffened shells in which the stiffener spacing is small enough for the shell to be approximated by a fictitious sheet whose orthotropic bending and extensional properties include those of the individual stiffening elements averaged out over representative widths or areas.

The behavior of the various types of orthotropic shells may be described by a single theory, the governing equations of which are equations of equilibrium for the buckled structure, and relationships between force and moment resultants and extensional and bending strains. The matrix equation relating the inplane forces and bending moments to the inplane strains and curvatures for shells of revolution with axes of orthotropy in the meridional and circumferential directions can be written in the following form:

$$\begin{Bmatrix} N_1 \\ N_2 \\ N_{12} \\ \\ M_1 \\ M_2 \\ M_{12} \end{Bmatrix} = \begin{bmatrix} C_{11} & C_{12} & 0 & C_{14} & C_{15} & 0 \\ C_{12} & C_{22} & 0 & C_{24} & C_{25} & 0 \\ 0 & 0 & C_{33} & 0 & 0 & 0 \\ & & & & & \\ C_{14} & C_{24} & 0 & C_{44} & C_{45} & 0 \\ C_{15} & C_{25} & 0 & C_{45} & C_{55} & 0 \\ 0 & 0 & 0 & 0 & 0 & C_{66} \end{bmatrix} \begin{Bmatrix} \epsilon_1 \\ \epsilon_2 \\ \epsilon_{12} \\ \\ \kappa_1 \\ \kappa_2 \\ \kappa_{12} \end{Bmatrix} \tag{16}$$

Zero entries in the above matrix generally refer to coupling terms for layers whose individual principal axes of stiffnesses are not aligned in meridional and circumferential directions. The values of the various elastic constants used in determining buckling loads of orthotropic shells are different for different types of construction. Some widely used expressions are given in reference 3.

The theory for single-layered shells of orthotropic material is similar to that for isotropic shells since the coupling terms C_{14}, C_{15}, C_{24}, and C_{25} may be set equal to zero. For stiffened doubly curved shells or for shells having multiple orthotropic layers, this is not generally possible and it is shown in references 38 and 39 that the neglect of coupling terms can lead to serious errors. For example, the inclusion of coupling terms yields a significant difference in theoretical results for stiffened shallow spherical-dome configurations having stiffeners on the inner surface or on the outer surface. The difference vanishes when coupling is neglected.

Very little theoretical or experimental data are available for orthotropic and stiffened doubly curved shells. General instability loads of pressurized shallow spherical domes with meridional stiffeners are determined in reference 40, and a semiempirical design formula is given in reference 41 for stiffened spherical caps. This formula closely approximates the test data given in reference 41. Buckling loads are given for grid-stiffened spherical domes in reference 42; references 40 to 42 do not include the effect of stiffener eccentricity.

Stiffener-eccentricity effects are investigated in reference 38 for grid-stiffened spherical domes. Eccentrically stiffened shallow equatorial toroidal shells under axial load and uniform pressure are investigated in reference 43. Reference 3 discusses the development of a buckling computer program that includes coupling as well as nonlinear prebuckling bending effects for orthotropic shells of revolution. (The cards and a computer listing for this program are available from COSMIC, University of Georgia, Athens, Georgia.) Numerical results obtained from this program, given in reference 3, were in good agreement with selected experimental results. The computer program can be used to determine the buckling load of the following orthotropic shells:

- Shells with ring and stringer stiffening.
- Shells with skew stiffeners.
- Fiber-reinforced (layered) shells.
- Layered shells (isotropic or orthotropic).
- Corrugated ring-stiffened shells.
- Shells with one corrugated and one smooth skin (with rings).

Boundary conditions may be closed at one or both ends, or may be free, fixed, or elastically restrained. Edge rings are permitted on the boundary.

This computer program can be used in conjunction with experimentally determined correlation factors to obtain buckling loads for orthotropic shells of revolution. The limitations of the program are given in reference 3.

The design recommendations given below are limited to spherical domes; the recommendations should also be verified by test, where feasible. The possibility of local buckling of the shell between stiffening elements should be checked.

The investigation of reference 42 gives the theoretical buckling pressure of a grid-stiffened spherical dome under uniform external pressure. This analysis assumes that the spherical dome is "deep" and that it contains many buckle wavelengths. In this case, the boundary conditions have little effect on the buckling load. Eccentricity effects are neglected. Experimental results given in reference 29 tend to support the assumptions of the analysis.

If the analysis of reference 42 is extended to the materially or geometrically orthotropic shell, then the hydrostatic buckling pressure can be expressed as

$$\frac{pR^3}{C_{44}\,\psi_1^{\frac{1}{2}}} = 4\gamma \left(\frac{1 + 2\,\frac{(C_{45} + C_{66})}{C_{44}} + \frac{C_{55}}{C_{44}}}{1 + \frac{C_{22}}{C_{11}} + 2\frac{C_{22}}{\psi_2}} \right)^{\frac{1}{2}} \tag{17}$$

where

$$\psi_1 = \frac{C_{22}R^2}{C_{44}} \left(1 - \frac{C_{12}^{\,2}}{C_{11}C_{22}} \right) \tag{18a}$$

$$\psi_2 = \frac{2C_{33}}{\left[1 - \frac{C_{12}^{\,2}}{C_{11}C_{22}} - 2\frac{C_{12}C_{33}}{C_{11}C_{22}} \right]} \tag{18b}$$

The constants C_{11} , C_{12} , C_{22} , C_{33} , C_{44} , C_{45} , C_{55} , and C_{66} are defined in reference 3 for the various materially and geometrically orthotropic materials. Equation (17) does not include the effect of stiffener eccentricity since the coupling terms C_{14} , C_{15} , C_{24} , and C_{25} in equation (16) have been neglected. Only limited experimental data exist for geometrically or materially orthotropic spherical domes subjected to hydrostatic pressure (refs. 29 and 41). In the absence of more extensive test results, it is recommended that the isotropic spherical cap reduction factor shown in equation (4) also be used for the orthotropic spherical shell. The correlation factor is given by

$$\gamma = 0.14 + \frac{3.2}{\lambda^2} \tag{19}$$

This equation is plotted in figure 2. The effective shell thickness to be used in obtaining λ is recommended as

$$t = \sqrt[4]{\frac{C_{44}C_{55}}{C_{11}C_{22}}}\ \sqrt{12} \qquad (20)$$

4.4 Isotropic Sandwich Doubly Curved Shells

The term "isotropic sandwich" designates a layered construction formed by bonding two thin isotropic facings to a thick core. Generally, the thin isotropic facings provide nearly all the bending rigidity of the construction; the core separates the facings and transmits shear so that the facings bend about a common neutral axis.

Sandwich construction should be checked for two possible modes of instability failure: (1) general instability failure where the shell fails with core and facings acting together, and (2) local instability failure taking the form of dimpling of the faces or wrinkling of the faces (fig. 19).

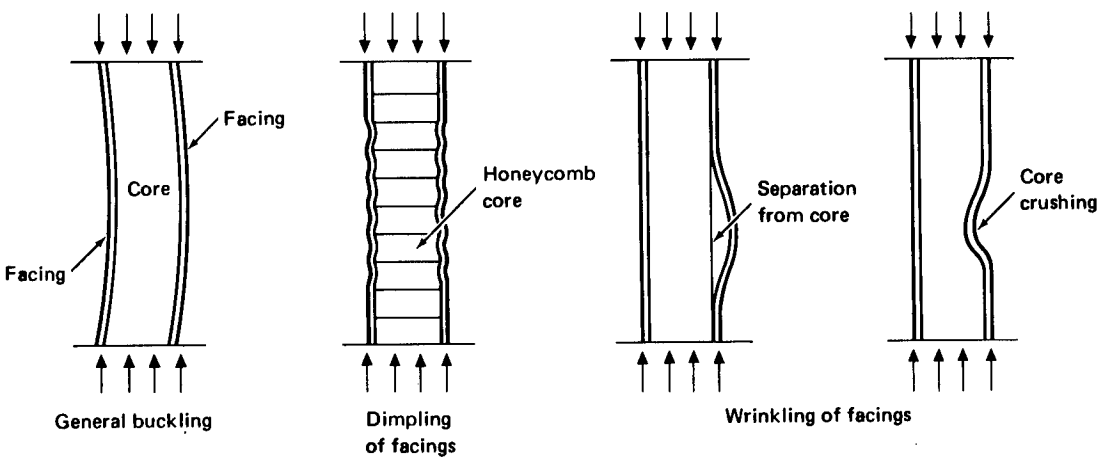

Figure 19
Types of failure of sandwich shells

4.4.1 General Failure

If the sandwich core is resistant to transverse shear so that its shear stiffness can be assumed to be infinite, the sandwich shell can be treated as an equivalent isotropic shell. For unequal thickness facings, the equivalent isotropic material thickness and modulus of elasticity are then given by

$$\bar{t} = \frac{\sqrt{12}h}{\sqrt{\frac{E_1 t_1}{E_2 t_2}} + \sqrt{\frac{E_2 t_2}{E_1 t_1}}} \tag{21a}$$

$$\bar{E} = \frac{E_1 t_1 + E_2 t_2}{\bar{t}} \tag{21b}$$

and for equal-thickness facings with the same modulus of elasticity, by

$$\bar{t} = \sqrt{3}\,h \tag{22a}$$

$$\bar{E} = \frac{2Et_f}{\sqrt{3}\,h} \tag{22b}$$

These equivalent properties can be used in conjunction with the recommended practices in Section 4.2 and with the computer program of reference 3 to analyze isotropic sandwich doubly curved shells.

Only one theoretical investigation which includes shear flexibility is available. Reference 44 treats the buckling of a sandwich sphere comprised of a core layer of low-modulus material and two equal facing layers of high-modulus material. Because there are insufficient theoretical and experimental data, no design recommendations can be given for this case.

4.4.2 Local Failure

Modes of failure other than overall buckling are possible. For honeycomb-core sandwich shells, failure may occur because of core crushing, intracell buckling, and face wrinkling. The use of relatively heavy cores ($\delta > 0.03$) will usually insure against core crushing. Lighter cores may prove to be justified as data become available. Procedures for the determination of intracell buckling and face-wrinkling loads are given in reference 45.

REFERENCES

1. Anon: Buckling of Thin-Walled Circular Cylinders. NASA Space Vehicle Design Criteria (Structures), NASA SP-8007, revised 1968.

2. Anon: Buckling of Thin-Walled Truncated Cones. NASA Space Vehicle Design Criteria (Structures), NASA SP-8019, 1968.

3. Almroth, B.O.; Bushnell D.; and Sobel, L.H.: Buckling of Shells of Revolution with Various Wall Constructions. Vols. I-III, NASA CR-1049 to CR-1051, 1968.

4. Ball, R.E.: A Geometrically Nonlinear Analysis of Arbitrarily Loaded Shells of Revolution. NASA CR-909, 1968.

5. Koiter, W.T.: Elastic Stability and Post-Buckling Behavior. Proc. Symp. Nonlinear Problems (edited by R.E. Langer), Univ. of Wisc. Press, 1963, p. 257.

6. Budiansky, B.; and Hutchinson, J.W.: Dynamic Buckling of Imperfection-Sensitive Structures. Proc. Eleventh International Congress of Applied Mechanics (edited by H. Gortler), Springer-Verlag (Berlin), 1964, pp. 636-651.

7. Fitch, J.R.: The Buckling and Post-Buckling Behavior of Spherical Caps Under Concentrated Load. Int. J. Solids Structures, vol. 4, no. 4, Apr. 1968, pp. 421-446.

8. Danielson, D.A.: Buckling and Initial Postbuckling Behavior of Spheroidal Shells Under Pressure. AIAA J., vol. 7, no. 5, May 1969, pp. 936-944.

9. Weinitschke, H.: On the Stability Problem for Shallow Spherical Shells. J. Math. and Phys., vol. 38, no. 4, Dec. 1960, pp. 209-231.

10. Budiansky, B.: Buckling of Clamped Shallow Spherical Shells. Proc. IUTAM Symposium on Theory of Thin Elastic Shells, North-Holland Publishing Co. (Amsterdam), 1960, pp. 64-94.

11. Huang, N.C.: Unsymmetrical Buckling of Thin Shallow Spherical Shells. J. Appl. Mech., vol. 31, no. 3, Sept. 1964, pp. 447-457.

12. Weinitschke, H.: On Asymmetric Buckling of Shallow Spherical Shells. J. Math. and Phys., vol. 44, no. 2, June 1965, pp. 141-163.

13. Thurston, G.A.; and Penning, F.A.: Effect of Axisymmetric Imperfections on the Buckling of Spherical Caps Under Uniform Pressure. AIAA J., vol. 4, no. 2, Feb. 1966, p. 319.

14. Bushnell, D.: Nonlinear Axisymmetric Behavior of Shells of Revolution. AIAA J., vol. 5, no. 3, Mar. 1967, pp. 432-439.

15. Wang, L.R.L.: Effects of Edge Restraint on the Stability of Spherical Caps. AIAA J., vol. 4, no. 4, Apr. 1966, pp. 718-719.

16. Bushnell, D.: Buckling of Spherical Shells Ring-Supported at the Edges. AIAA J., vol. 5 no. 11, Nov. 1967, pp. 2041-2046.

17. Wang, L.R.L.: Discrepancy of Experimental Buckling Pressures of Spherical Shells. AIAA J., vol. 5, no. 2, Feb. 1967, pp. 357-359.

18. McComb, H.G., Jr. ; and Fitcher, W.B.: Buckling of a Sphere of Extremely High Radius-Thickness Ratio. Collected Papers on Instability of Shell Structures, NASA TN D-1510, 1962, pp. 561-570.

19. Mescall, J.F.: Large Deflections of Spherical Shells Under Concentrated Loads. J. Appl. Mech., vol. 32, no. 4, Dec. 1965, pp. 936-938.

20. Bushnell, D.: Bifurcation Phenomena in Spherical Shells Under Concentrated and Ring Loads. AIAA J., vol. 5, no. 11, Nov., 1967, pp. 2034-2040.

21. Ashwell, D. G.: On the Large Deflection of a Spherical Shell With an Inward Point Load. Proc. IUTAM Symposium on the Theory of Thin Elastic Shells, North-Holland Publishing Co. (Amsterdam), 1960, pp. 43-63.

22. Evan-Iwanowski, R.M.; Cheng, H.S.; and Loo, T.C.: Experimental Investigations and Deformation and Stability of Spherical Shells Subjected to Concentrated Loads at the Apex. Proc. Fourth U.S. Nat. Engr. Appl. Mech., 1962, pp. 563-575.

23. Penning, F.A.; and Thurston, G.A.: The Stability of Shallow Spherical Shells Under Concentrated Load. NASA CR-265, 1965.

24. Penning, F.A.: Experimental Buckling Modes of Clamped Shallow Shells Under Concentrated Load. J. Appl. Mech., vol. 33, no. 2, June 1966, pp. 297-304.

25. Penning, F.A.: Nonaxisymmetric Behavior of Shallow Shells Loading at the Apex. J. Appl. Mech., vol. 33, no. 3, Sept. 1966, pp. 699-700.

26. Loo, T.C.; and Evan-Iwanowski, R.M.: Interaction of Critical Concentrated Loads Acting on Shallow Spherical Shells. J. Appl. Mech., vol. 33, no. 3, Sept. 1966, pp. 612-616.

27. Hyman, B.I.; and Healey, J.J.: Buckling of Prolate Spheroidal Shells Under Hydrostatic Pressure. AIAA J., vol. 5, no. 8, Aug. 1967, pp. 1469-1477.

28. Nickell, E.H.: Experimental Buckling Tests of Magnesium Monocoque Ellipsoidal Shells Subjected to External Hydrostatic Pressure. Tech. Rept. 3-42-61-2, Vol. IV, Lockheed Missiles & Space Co., June 30, 1961.

29. Meyer, R.R.; and Bellinfante, R.J.: Fabrication and Experimental Evaluation of Common Domes Having Waffle-like Stiffening. Rept. SM-47742, Douglas Aircraft Company, Inc., 1964.

30. Thurston, G.A.; and Holston, A.E., Jr.: Buckling of Cylindrical Shell End Closures by Internal Pressure. NASA CR-540, 1966.

31. Adachi, J.; and Benicek, M.: Buckling of Torispherical Shells Under Internal Pressure. Exp. Mech., vol. 4, no. 8, Aug. 1964, pp. 217-222.

32. Sobel, L.H.; and Flügge, W.: Stability of Toroidal Shells Under Uniform External Pressure. AIAA J., vol. 5, no. 3, Mar. 1967, pp. 425-431.

33. Hutchinson, J.W.: Initial Post-Buckling Behavior of Toroidal Shell Segments. Int. J. Solids Structures, vol. 3 no. 1, Jan. 1967, pp. 97-115.

34. Yao, J.C.: Buckling of a Truncated Hemisphere Under Axial Tension. AIAA J., vol. 1, no. 10, Oct. 1963, pp. 2316-2320.

35. Babcock, C.D., and Sechler, E.E.: The Effect of Initial Imperfections on the Buckling Stress of Cylindrical Shells. Collected Papers on Instability of Shell Structures. NASA TN D-1510, 1962, pp. 135-142.

36. Blum, R.E.; and McComb, H.G., Jr.: Buckling of an Equatorial Segment of a Spherical Shell Loaded by its Own Weight. NASA TN D-4921, 1968.

37. Stein, M.; and McElman, J.A.: Buckling of Segments of Toroidal Shells. AIAA J., vol. 3, no. 9, Sept. 1965, pp. 1704-1709.

38. Crawford, R.F.: Effects of Asymmetric Stiffening on Buckling of Shells. AIAA Paper no. 65-371, 1965.

39. Bushnell, D.: Symmetric and Nonsymmetric Buckling of Finitely Deformed Eccentrically Stiffened Shells of Revolution. AIAA J., vol. 5, no. 8, Aug. 1967, pp. 1455-1462.

40. Ebner, H.: Angeneherte Bestimmung der Tragfähigkeit radial versteifter Kugelschalen unter Druckbelastung. Proc. IUTAM Symposium on the Theory of Thin Elastic Shells, North-Holland Publishing Co. (Amsterdam), 1960, pp. 95-121.

41. Klöppel, K.; and Jungbluth, O.: Beitrag zum Durchschlagproblem dünnwandiger Kugelschalen. Der Stahlbau, Vol. VI. 1953, pp. 121-130. (Also available as David Taylor Model Basin Translation 308, May 1966.)

42. Crawford, R.F.; and Schwartz, D.B.: General Instability and Optimum Design of Grid-Stiffened Spherical Domes. AIAA J., vol. 3, no. 3, Mar. 1965, pp. 511-515.

43. McElman, J.A.: Eccentrically Stiffened Shallow Shells of Double Curvature. NASA TN D-3826, Feb. 1967.

44. Yao, J.C.: Buckling of Sandwich Sphere Under Normal Pressure. J. Aerospace Sci., vol. 29, no. 3, Mar. 1962, pp. 264-268.

45. Anon: Structural Sandwich Composites. MIL-HDBK 23, Dec. 30, 1968.

SYMBOLS

a	radius of curvature of circular toroidal-shell cross section (See fig. 13.)
b	distance from center of circular cross section of circular toroidal-shell cross section to axis of revolution (See fig. 13.)
A,B	lengths of semiaxes of ellipsoidal shells
C_{ij}	coefficients of constitutive equations [See eq. (16).]
D	monocoque shell-wall flexural stiffness, $\frac{Et^3}{12(1-\mu^2)}$
E	Young's modulus
$\bar{E}$	equivalent Young's modulus for isotropic sandwich shells
E_1,E_2	Young's moduli of the 1- and 2-face sheets, respectively, for isotropic sandwich shells
h	distance between middle surfaces of the top and bottom face sheets for isotropic sandwich shells
ℓ	length of toroidal-shell segment (See fig. 18.)
M_1,M_2,M_{12}	moment resultants per unit of middle surface length
N	axial tension force per unit circumference applied to a toroidal segment (See fig. 15.)
N_1,N_2,N_{12}	force resultants per unit of middle surface length
n	number of buckle waves in the circumferential direction
P	concentrated load at apex of spherical cap
P_{cr}	critical concentrated load at apex of spherical cap
p	uniform pressure
$p_{c\ell}$	classical uniform buckling pressure for a complete spherical shell
p_{cr}	critical uniform pressure
R	radius of spherical shell
R_A	effective radius of a thin-walled oblate spheroid, $\frac{B^2}{A}$
R_c	maximum radius of torispherical shell (See fig. 11.)
R_t	toroidal radius of torispherical shell (See fig. 11.)
r	radius of equator of toroidal shell segment (See fig. 18.)
t	thickness of single-layered shell
$\bar{t}$	equivalent constant thickness for isotropic sandwich shells [See eq. (21).]
t_f	face thickness of sandwich shell having equal-thickness faces

t_1, t_2	face-sheet thicknesses for sandwich construction having faces of unequal thickness
Z	curvature parameter of toroidal-shell segment, $\sqrt{(1-\mu^2)}\ \frac{\ell^2}{rt}$
β	buckle wavelength parameter, $\frac{n\ell}{\pi r}$
γ	correlation factor to account for difference between classical theory and recommended lower-bound instabiliy loads
δ	ratio of core density of honeycomb sandwich to density of face sheet
$\epsilon_1, \epsilon_2, \epsilon_{12}$	reference-surface strains
$\kappa_1, \kappa_2, \kappa_{12}$	reference-surface curvature changes
λ	spherical-cap geometry parameter [See eq. (3).]
μ	Poisson's ratio
ϕ	half the included angle of spherical cap (See fig. 1.)
ϕ_0	half the included angle of spherical cap portion of torispherical closure (See fig. 11.)
ψ_1, ψ_2	[See eq. (18).]

NASA SPACE VEHICLE DESIGN CRITERIA MONOGRAPHS ISSUED TO DATE

SP-8001	(Structures)	Buffeting During Launch and Exit, May 1964
SP-8002	(Structures)	Flight-Loads Measurements During Launch and Exit, December 1964
SP-8003	(Structures)	Flutter, Buzz, and Divergence, July 1964
SP-8004	(Structures)	Panel Flutter, May 1965
SP-8005	(Environment)	Solar Electromagnetic Radiation, June 1965
SP-8006	(Structures)	Local Steady Aerodynamic Loads During Launch and Exit, May 1965
SP-8007	(Structures)	Buckling of Thin-Walled Circular Cylinders, September 1965 – Revised August 1968
SP-8008	(Structures)	Prelaunch Ground Wind Loads, November 1965
SP-8009	(Structures)	Propellant Slosh Loads, August 1968
SP-8010	(Environment)	Models of Mars Atmosphere (1967), May 1968
SP-8011	(Environment)	Models of Venus Atmosphere (1968), December 1968
SP-8012	(Structures)	Natural Vibration Modal Analysis, September 1968
SP-8013	(Environment)	Meteoroid Environment Model – 1969 [Near Earth to Lunar Surface], March 1969
SP-8014	(Structures)	Entry Thermal Protection, August 1968
SP-8015	(Guidance and Control)	Guidance and Navigation for Entry Vehicles, November 1968
SP-8016	(Guidance and Control)	Effects of Structural Flexibility on Spacecraft Control Systems, April 1969
SP-8017	(Environment)	Magnetic Fields – Earth and Extraterrestrial, March 1969
SP-8018	(Guidance and Control)	Spacecraft Magnetic Torques, March 1969
SP-8019	(Structures)	Buckling of Thin-Walled Truncated Cones, September 1968
SP-8020	(Environment)	Mars Surface Models [1968], May 1969
SP-8021	(Environment)	Models of Earth's Atmosphere (120 to 1000 km), May 1969
SP-8023	(Environment)	Lunar Surface Models, May 1969
SP-8024	(Guidance and Control)	Spacecraft Gravitational Torques, May 1969
SP-8029	(Structures)	Aerodynamic and Rocket-Exhaust Heating During Launch and Ascent, May 1969
SP-8031	(Structures)	Slosh Suppression, May 1969

NASA-Langley, 1970 —— 32